Desalination and Water Treatment
www.deswater.com
doi: 10.5004/dwt.2022.28447

259 (2022) 1–16
May

Mitigating salt accumulation in osmotic membrane bioreactors using ion-exchange resins

Hui Zhang[a], Jinrong Liu[a], Hongwei Song[b,*]

[a]*School of Chemical Engineering, Inner Mongolia University of Technology, Hohhot 010051, China, emails: 1911895102@qq.com (H. Zhang), jinrong_liu@126.com (J. Liu)*
[b]*School of Civil Engineering, Inner Mongolia University of Technology, Hohhot 010051, China, email: songhongwei_8112@163.com*

Received 29 November 2021; Accepted 27 March 2022

ABSTRACT

Osmotic membrane bioreactor (OMBR) is an emerging technology with great potentials for wastewater treatment and resource utilization. Nevertheless, salinity build-up is still one of main obstacles of OMBR development. In this paper, an OMBR system was combined with a membrane distillation (MD) system to recycle wastewater and an IERs-OMBR-MD hybrid system was developed to mitigate the salt accumulation in bioreactors. Water flux, water quality, properties of activated sludge and membrane fouling were investigated. The results show that the ion-exchange resins (IERs) dosage of 8 g/L can keep a conductivity of 6.87 mS/cm in the bioreactor during 30 d of operation, which was 30% lower than the conductivity in a traditional osmotic membrane bioreactor-membrane distillation (OMBR-MD) without adding the IERs. A water flux difference of about 58% was found between the OMBR-MD system (1.135 L/(m^2 h)) and the IERs-OMBR-MD system (2.675 L/(m^2 h)) after 30 d of operation. The IERs-OMBR-MD produced significantly less fouling to the forward osmosis membrane than the traditional OMBR-MD. We suggest that IERs can be used to absorb soluble salts to mitigate salinity build-up in OMBRs operation. Overall, the IERs-OMBR-MD hybrid system has the potential to recycle wastewater. However, it is necessary to further improve the long-term stability of activated sludge in OMBRs.

Keywords: Osmotic membrane bioreactor; Ion-exchange resins; Salt accumulation; Membrane fouling; Wastewater recycling

1. Introduction

Rapid population growth and accelerated industrialization have increased the demand for clean water, greatly reducing the limited freshwater resources. Water safeguard has been a tactical matter related to the national stability and socioeconomic development of a country [1–3]. Membrane separation technology, due to its high efficiency and easy operation, plays a direct and effective role in alleviating water shortage and water pollution [4,5]. Its popularity relative to conventional activated sludge (CAS) methods is due to several distinctive advantages such as allowing high sludge concentrations, low sludge yield, producing high quality effluent and with small occupation area. Unfortunately, membrane bioreactor (MBR) is challenged by the higher investment cost and serious membrane fouling, as well as its relatively high energy consumption due to the hydraulic pressure applied for separation [6,7]. Forward osmosis (FO) is an emerging membrane separation technology, which has great application prospects in solving water shortage [8–11]. An osmotic membrane bioreactor-membrane distillation (OMBR-MD) hybrid system is a combination of FO, activated sludge process and a draw solution (DS) recovering system.

* Corresponding author.

Membrane distillation (MD) can reconcentrate the diluted DS to produce high quality water. MBR uses microfiltration (MF) or ultrafiltration (UF) membranes, driven by external pressure, whereas osmotic membrane bioreactor (OMBR) uses dense FO membranes, driven by osmotic pressure difference [12–14]. Therefore, compared with MBR, OMBR has lower membrane fouling tendency, higher quality effluent and lower energy consumption. However, there are inherent problems with this technology. For instance, the high rejection of the FO membrane causes the accumulation of dissolved salts in bioreactors. Salt accumulation can reduce osmotic driving force, decrease water flux, aggravate membrane fouling, degrade membrane performance, and inhibit or poison microbial diversity and activity in bioreactors [15–17].

In previous studies, in order to mitigate the salt build-up in the OMBR, a number of hard works have been put into the choice of draw solutes (DS) [18–22] and invention of an ideal FO membrane [23,24]. In addition, sludge retention time (SRT) has been deemed to be a practicable method to control the salt accumulation in the OMBR through regular sludge discharge. However, the shorter SRT results in the lower sludge concentrations, for example, the mixed liquor suspended solids (MLSS) in the OMBR system decreased to 1.02 ± 0.10 g/L at the 10th day, which may degrade OMBR performance [25,26]. Therewith, some researches combined microfiltration (MF) [27–29] and ultrafiltration (UF) [14,30] with the OMBR. The supernatant containing salts may be separated from the OMBR through a MF or UF membrane cell but the water flux of the MF or UF is lower than the expected due to the increase of filtration resistance and external concentration polarization (ECP). Lu and He [31] proposed a hybrid OMBR-electrodialysis (ED) system to alleviate salt accumulation. The introduction of the ED technology could keep the low conductivity in the bioreactor. With the applied voltage of 3 V, the conductivity reached 1.6 mS/cm within 24 h, which was about 2.3 times longer than during that in the conventional OMBR. Viet et al. [32] designed a novel hybrid configuration of an osmotic membrane bioreactor-clarifier (OMBRC) to achieve the simultaneous decrease of the salt accumulation and membrane fouling. Nevertheless, the further disposal of the extracted supernatant containing a high concentration of salts will be challenging. Ion-exchange resins (IERs) will be used to solve the problems mentioned for the first time in this study.

IERs are functional polymers with crosslinked macromolecular skeletons. Ionized groups on the skeletons can adsorb molecules through ion-exchange reactions [33]. The adsorption mechanism is that H^+ and OH^- are dissociated from the main functional groups ($R\text{-}SO_3H$, $R\text{-}N(CH_3)_3OH$) in IERs to form positive and negative groups, which can combine with the cations or anions in water to remove the target ions. IERs are mainly used in the preparation of pure water, the treatment of wastewater and the extraction of biochemical products [34–36]. In this study, for the first time, a system combining an OMBR with IERs was established. In this IERs-OMBR system, the IERs were added to the bioreactor to alleviate salinity bulid-up. This study aims to evaluate the performances of the IERs-OMBR-MD hybrid system during 30 d of operation, and compared it with a traditional OMBR-MD system in terms of water flux, conductivity, water quality, properties of activated sludge and membrane fouling. The rework offers readers with a broader understanding of the value of IERs. Results reported here can provide significant insights to mitigate salt accumulation in OMBRs.

2. Materials and methods

2.1. Feed and draw solutions

The activated sludge collected from a wastewater treatment plant in Hohhot (Inner Mongolia, China) was used as the inoculum for the OMBR system. Before being used in the OMBR, the activated sludge was cultivated for 3 months with synthetic domestic wastewater (Table S1). The synthetic domestic wastewater was also used as the influent for two OMBR-MD systems. The mixed liquor in the bioreactor (BR) was the feed solution (FS). The draw solution (DS) was prepared using 58.45 g analytical grade sodium chloride (NaCl) dissolved in 1 L deionized water.

2.2. Experimental set-up

A lab-scale OMBR-MD hybrid system was used in this experiment (Fig. 1). The hybrid system included a domestic wastewater reservoir, a bioreactor (BR), an external FO membrane cell, a draw solution (DS) reservoir, an MD module and a cooling water reservoir.

The effective volume of the BR was 4.5 L, maintaining a constant liquid level through a controller. The domestic wastewater reservoir was placed on a precise balance, and the FO water flux was calculated by the weight changes of the balance. A flat-frame FO membrane cell made of polymethylmethacrylate was placed outside the BR. A flat-sheet, cellulose triacetate (CTA) FO membrane was supplied by Hydration Technology Innovations (HTI, Albany, NY, USA) and its active layer faced the FS (AL-FS mode). The effective area of FO membrane was 90 cm^2. Two peristaltic pumps were used to circulate the DS and mixed liquor respectively from the DS reservoir and BR to the two sides of the FO membrane cell both at a cross-flow velocity of 120 rpm.

The MD module was composed of three hot chambers and four cooling water chambers, and the distance between each pair of two cold and hot chambers was 3 mm. The MD membrane was polytetrafluoroethylene (PTFE) material and had a total effective membrane area of 600 cm^2. Two peristaltic pumps were used to circulate the DS and cooling water respectively from two reservoirs to the MD module both at a cross-flow velocity of 300 rpm. The DS was controlled at 35°C by a thermostatic water bath. The cooling water was kept at 13°C–15°C. The diluted DS was condensed through the MD module to maintain a stable driving force on both sides of the FO membrane.

2.3. Experimental protocol

An IERs-OMBR-MD and a traditional OMBR-MD hybrid systems were set up to compare the operational performances. The only difference between two systems was the

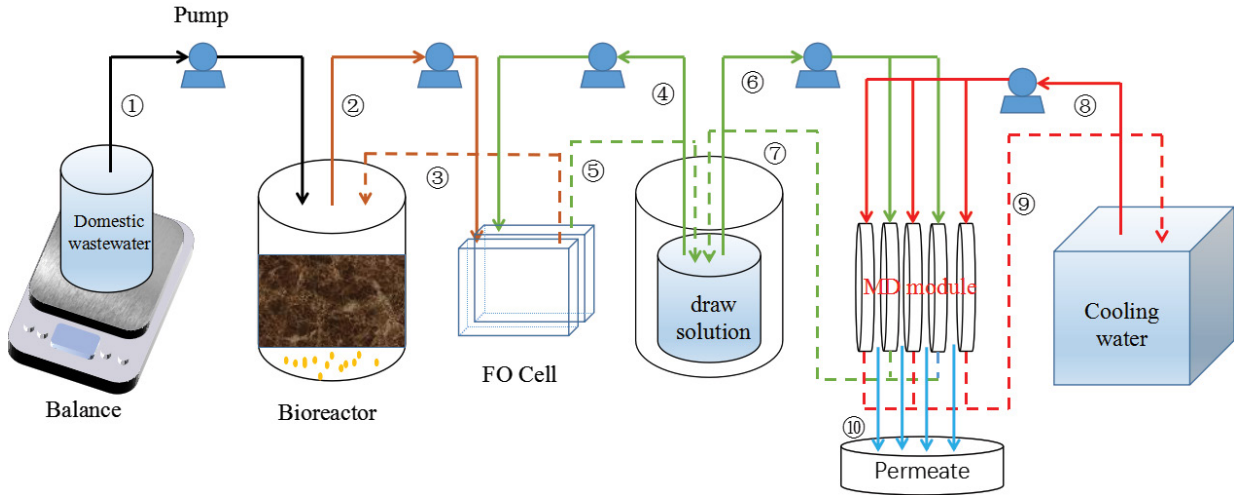

Fig. 1. Schematic diagram of the OMBR-MD experiment. ① Domestic wastewater flows to the BR; ② Sludge mixture flows to the active layer side of the FO cell; ③ Sludge mixture flows back into the BR; ④ DS flows to the supporting layer side of the FO cell; ⑤ DS flows back into the DS tank; ⑥ DS flows to the hot chambers of the MD module; ⑦ DS in the MD module flows back into the DS tank; ⑧ Cooling water flows to the cold chambers of the MD module; ⑨ Cooling water flows back into the cooling water tank; ⑩ MD permeate.

addition of mixed ion-exchange resins during the first 10 d and the last 10 d of the IERs-OMBR-MD operation to control the salinity in the BR. Since the salinity increased rapidly in the early stage of the OMBR experiment, the IERs were added to control salinity and maintain system flux during the first 10 d of the operation period. During the last 10 d, the IERs were re-added to validate the recovering effects of the system after the middle 10 d operation without the IERs. In order to characterize and recycle the IERs, the IERs were wrapped with non-woven cloth and added to the bioreactor, and after 24 h adsorption, the IERs were taken out timely for recycling and characterization, instead the fresh IERs were added to the bioreactor.

The OMBR experiment period was set to be 30 d. The BR was constantly aerated to hold the dissolved oxygen (DO) concentration of 5 mg/L. The DS was 1 M NaCl solution, and the effective volume of the DS was 5 L. The BR temperature can be kept at about 27°C by circulating the DS (35°C) to the FO cell. The initial concentration of MLSS was adjusted to be 5.5 g/L. No sludge was discharged during 30 d of operation except for drawing a water sample of 100 mL mixed liquor every 5 d. By the IERs adsorption tests, the dosage of the mixed IERs were determined to be 8 g/L (Fig. S1), and the ratio of anion and cation exchange resins was 3:1 (Fig. S2). The mixed IERs were strong basic styrene anion exchange resins (201×7) and macroporous strong acid styrene cation exchange resins (D001). Before the experiment, 201×7 and D001 were pretreated with 1 M NaOH and 1 M HCl, respectively.

2.4. Analytical methods

2.4.1. Water flux

The weight of the domestic wastewater reservoir and the Cl^- concentration of the BR were recorded every hour. Briefly, the average of 24 h was taken as a cycle to obtain the daily water flux. The FO water flux, J_W (L/(m²·h), was defined as Eq. (1):

$$J_W = \frac{\Delta V}{A \cdot \Delta t} \tag{1}$$

where ΔV (L) is the water volume flowing through the FO membrane over the interval time Δt (h) and A (m²) is the effective FO membrane area.

Total removal efficiency of pollutants, R (%), is defined as Eq. (2):

$$R = \frac{C_{FS} - C_{MD}}{C_{FS}} \times 100\% \tag{2}$$

where C_{FS} (mg/L) and C_{MD} (mg/L) represent the contaminant concentrations of the influent (domestic wastewater) and effluent (MD permeate), respectively.

2.4.2. Water quality

Grab water samples were taken every other day from the domestic wastewater reservoir, the BR, the DS reservoir, and the MD permeate, respectively. The concentrations of total organic carbon (TOC) and total nitrogen (TN) were determined using a multi N/C 2100S TOC/TN analyzer (Analytik Jena, Germany). The concentrations of ammonium nitrogen (NH_4^+–N), labile phosphorus (PO_4^{3-}) and nitrate nitrogen (NO_3–N and NO_2–N) were measured following the standard means for the examination of water and wastewater 20th edition (APHA, 1998) using a UV-3150PC ultraviolet spectrophotometer (Shimadzu, Kyoto, Japan). The Cl^- concentration was measured using a PXSJ-226 ion meter (INESA, China). The mixed liquor pH value and conductivity were surveyed employing a PHSJ-3F pH meter (INESA, China) and a DDSJ-308A conductivity meter (INESA, China), respectively.

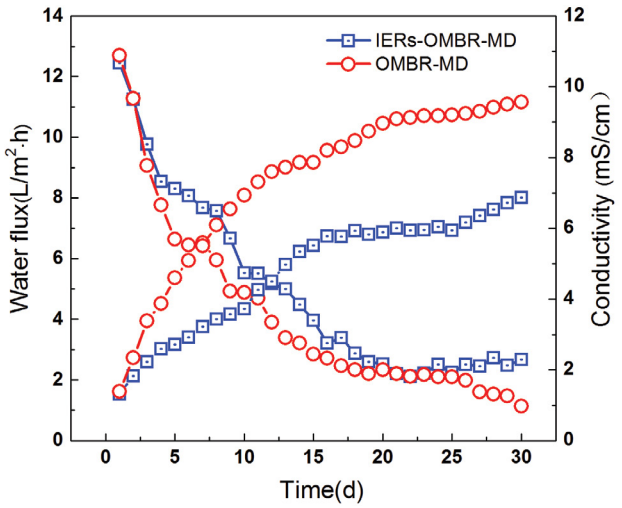

Fig. 2. Comparison of the IERs-OMBR-MD and OMBR-MD on water flux and conductivity.

2.4.3. Properties of activated sludge

Grab sludge samples were taken every 5 d from the BR. The concentrations of MLSS and mixed liquor volatile suspended solids (MLVSS) in the BR were determined following the standard means 2540 (APHA, 1998). Zeta potential was measured using a ZEN3690 Zeta potentiometric analyzer (Malvern, England). The specific oxygen uptake rate (SOUR) of activated sludge was measured using a ORION 3 STAR dissolved oxygen instrument (ThermoFisher Scientific, China). Soluble microbial products (SMP) were extracted through centrifugal rotation at 4,000 rpm for 5 min. The extraction of bound extracellular polymer substances (BEPS) needs to heat the mixed liquor using a water bath for 30 min [37,38]. The concentrations of SMP and BEPS in the mixed liquor can be obtained by testing the protein and polysaccharide contents totality using the Lowry method [39] and anthrone–sulfuric method [40], respectively.

2.4.4. Membrane fouling

The fouled FO membranes collected from the IERs-OMBR-MD and OMBR-MD hybrid system were further analyzed at the end of the experiment. The morphology and inorganic compositions were surveyed employing a NOVA NANOSEM 230 scanning electron microscopy (SEM) coupled to an energy-dispersive X-ray spectrometer (EDS X-MAX50) (FEI, USA). A Fourier-transform infrared (FTIR) spectrophotometer (Nexus 670, Nicolet, USA) was used to characterize the main functional groups of organic matters on the surface of the FO membrane. Contaminants on the FO membrane within an area of 2 cm × 2 cm were scraped and prepared into suspension solution, and the contents of TOC, polysaccharide and protein were analyzed.

2.4.5. Performances of the recovered IERs

The morphology and composition of the recovered IERs were also tested by SEM (NOVA NANOSEM 230). The IERs regeneration and recovery steps are as follows: (1) the IERs were taken out of the BR and immersed in deionized water for 6 h to wash away the pollutants on the IERs surface. (2) adding 0.7 mol/L NaOH solution twice the volume into the reclaimed 201×7 exchange resins, leaching and soaking for 6 h, then the alkali solution was poured out; the D001 exchange resins was added with 0.7 mol/L HCl solution twice the volume, rinsed and soaked for 6 h, then the acid solution was poured out, and both resins were washed to be neutral with deionized water. (3) The regenerated IERs were dried in a constant temperature oven at 40°C for next use. The static adsorption effects of the reclaimed resins with different initial concentrations of NaCl solutions (100, 200, 300, 400, 500, 600, 700, 800, 900 and 1,000 mg/L) were tested.

3. Results and discussions

3.1. Water flux and salt accumulation

The water flux and conductivity in the bioreactors of the IERs-OMBR-MD and OMBR-MD system are shown in Fig. 2. The initial water fluxes of the IERs-OMBR-MD and OMBR-MD systems were 14.5 and 14.7 L/(m^2 h), respectively. At the beginning of the experiment, due to the rapid salt accumulation and membrane fouling, the fluxes of the two systems were severely attenuated and the water flux gap was small. However, since the 4th day of the experiment, the water flux of the IERs-OMBR-MD began to be higher than that of the OMBR-MD. After 20 d of operation, the water flux of the OMBR-MD system tended to be stable, but the re-addition of the IERs caused a slight increase in the water flux of the IERs-OMBR-MD system. A difference of about 58% was observed between the OMBR-MD system flux (1.135 L/(m^2 h)) and the IERs-OMBR-MD system value (2.675 L/(m^2 h)) after 30 d of operation. The reason may be that the IERs alleviated salt accumulation and increased the osmotic pressure of the OMBR system.

Salt accumulation is an inherent phenomenon related to OMBRs due to the high salt rejection by FO membranes and the reverse transportation of draw solutes [15]. The conductivity of the OMBR-MD system continually increased from about 1.3 to 9.57 mS/cm during the whole operation period. However, the conductivity of the IERs-OMBR-MD system only increased from 1.3 to 6.87 mS/cm, which was 30% lower than the salinity of the traditional OMBR-MD after 30 d of operation. Such low salt accumulation was attributed to the adsorption of anions (Cl^-, NO_3^-, PO_4^{3-}, etc.) and cations (Na^+, Ca^{2+}, K^+, etc.) in the BR by the resins 201×7 and D001. The dissociation of $[N^+(CH_3)_3OH^-]$ results in the formation of $[N(CH_3)_3]^+$ and $OH^-$and similar anions are adsorbed on the functional groups owing to differences in the affinity of the functional groups with electric charges towards different anions ($SO_4^{2-} > NO_3^- > Cl^- > OH^-$) [41,42]. The dissociation of $[SO_3H^+]$ results in the formation of $-SO_3^-$ and H^+ and similar cations are adsorbed on the functional groups owing to differences in the affinity of the functional groups with electric charges towards different cations ($Ca^{2+} > Mg^{2+} > K^+ > Na^+ > H^+$)[43]. Millar et al. reported a method of desalting coal seam water

using synthetic ion-exchange resins [44]. The higher conductivity in the BR resulted in the lower osmotic pressure difference on both sides of the FO membrane. As a result, the water flux of the IERs-OMBR-MD system was higher than that of the traditional OMBR-MD system. The flux decline and salinity build-up of OMBRs were also reported in previous papers [18,28,45].

3.2. Removals of bulk organic matters and nutrients

The removals of bulk organic matters and nutrients in the IERs-OMBR-MD and OMBR-MD hybrid system are shown in Figs. 3 and 4. As shown in Figs. 3a_1, a_2, TOC concentration in the BR increased slightly in the OMBR-MD system. This could be due to the negative impact on sludge concentration and activity by salt accumulation. In addition, the efficient rejection of the FO membrane also allowed the undegraded organic matters to be accumulated in the BR continuously. In contrast, TOC concentration in the IERs-OMBR-MD system was lower, because the IERs adsorbed soluble salts and organic matters in the BR, thus reducing salinity and membrane fouling.

As shown in Figs. 3b_1, b_2, the drastic TN accumulation occurred in the BR and DS during the operation of the OMBR-MD system due to the biological nitrification. Generally, nitrification converts NH_4^+–N to nitrite (NO_2–N) and then nitrate (NO_3–N) under aerobic conditions. The high concentration of TN in the DS, somewhere even higher than that in the BR, illustrated that the FO membrane allowed parts of TN to pass through. But, during the first and last 10 d of the IERs-OMBR system operation, the concentration of TN in the BR significantly decreased, which resulted from the adsorption of NO_3^- and NO_2^- by 201×7. The results can also be illustrated in Figs. 4b_1, c_1.

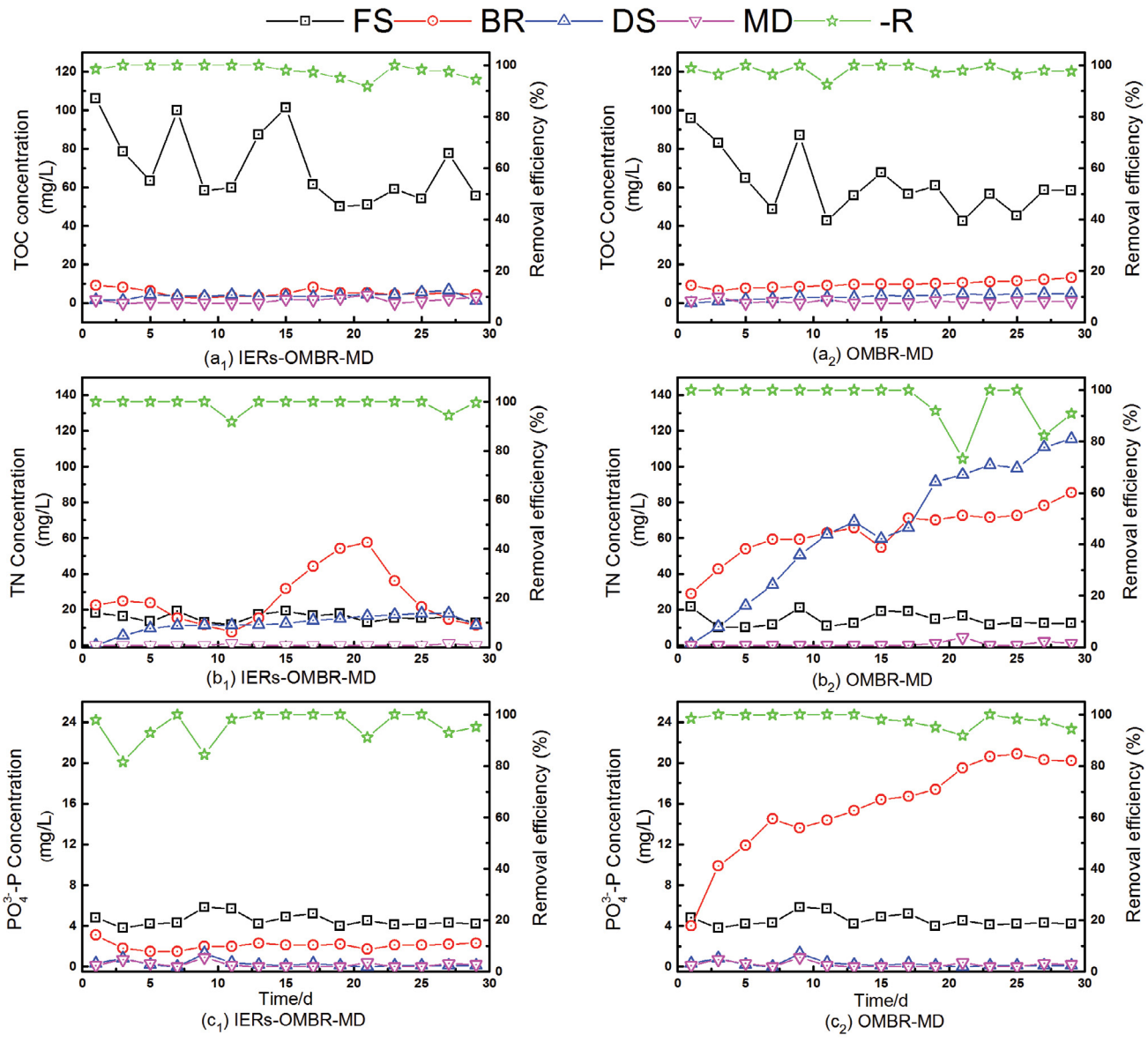

Fig. 3. TOC, TN and PO_4^{3-} concentrations in the IERs-OMBR-MD and OMBR-MD hybrid system.

Phosphorus removal by biological treatment relies on microbial assimilation, especially by phosphate accumulating microorganisms (PAOs). The activity of PAOs is vulnerable to saline environment, and a considerable reduction in phosphorus removal owing to salinity build-up was reported in previous literature [46]. Therefore, the high rejection of the FO membrane plays a dominant role in total phosphorus removal of two hybrid systems. Holloway et al. stated that FO membrane almost completely repels phosphate during concentration of anaerobic digester centrate, due to the fact that phosphate ions are negatively charged and have large hydrated radius [47]. As shown in Figs. 3c_1, c_2, the concentration of PO_4^{3-}–P continuously increased in the OMBR-MD system. By contrast, the concentration of PO_4^{3-}–P decreased in the IERs-OMBR-MD system during the first 10 d due to the adsorption of PO_4^{3-}–P in the BR by the 201×7 resins, and even during the period time without the addition of the IERs, the phosphorus accumulation rarely occurred probably due to the mitigation of salinity build-up.

As shown in Figs. 4a_1, a_2, the concentrations of NH_4^+–N in the BR and DS during the operation of both systems were low mainly because of complete nitrification. But the non-ignorable NH_4^+–N concentration in the MD indicates FO and MD membranes cannot reject NH_4^+–N efficiently.

Figs. 4b_1, b_2 show that the variation of NO_3–N was consistent with the variation of TN. Interestingly, the concentrations of TN were much higher than the concentrations of NO_3–N both in the BR and DS, indicating that organic nitrogen may be also present in the BR and DS besides NH_4^+–N, NO_2–N and NO_3–N. The accumulation of organic nitrogen in the BR and DS may be ascribed to the inhibition of high salinity on the ammonifying bacteria.

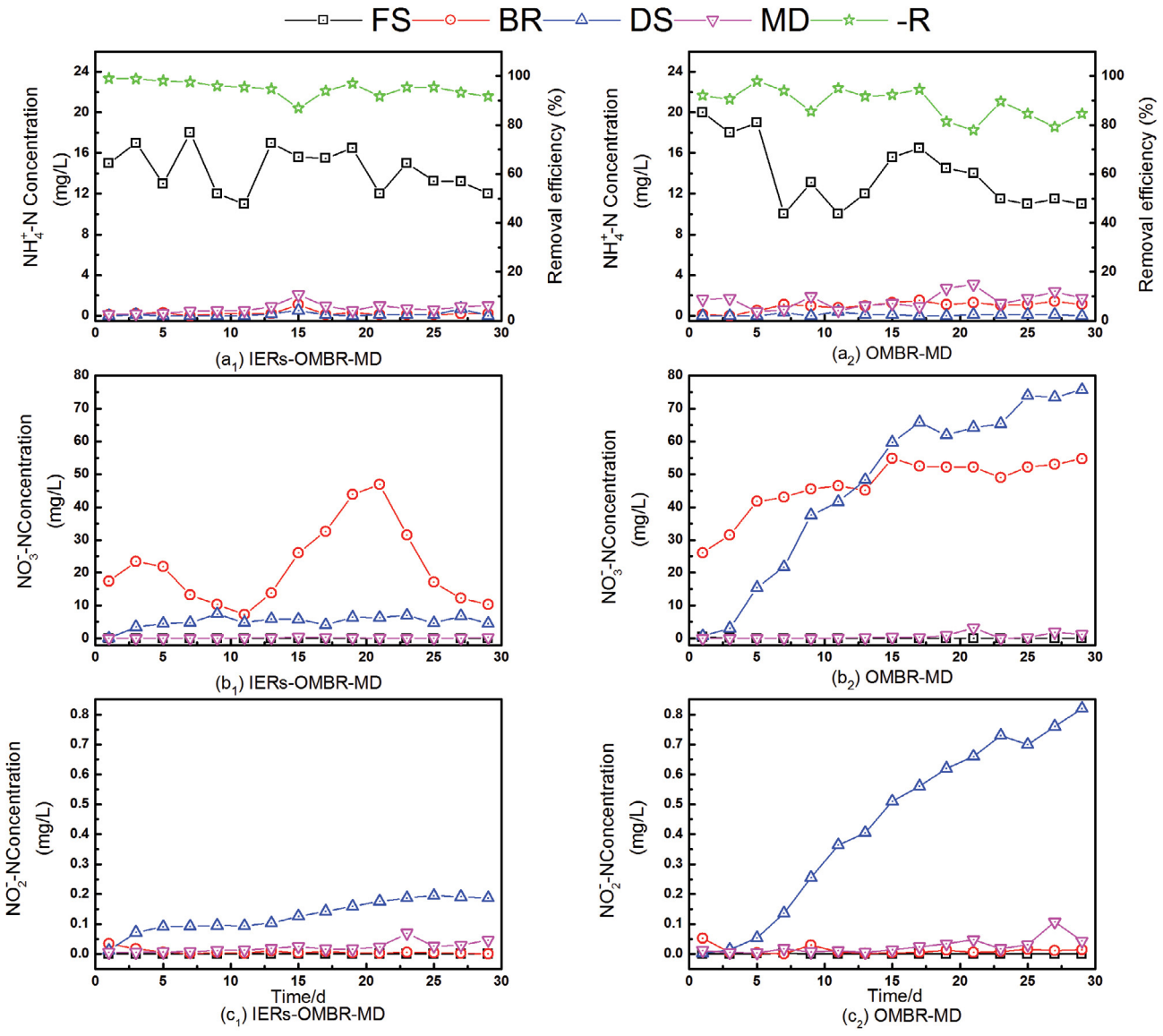

Fig. 4. NH_4^+–N, NO_3–N and NO_2–N concentrations in the IERs-OMBR-MD and OMBR-MD hybrid system.

As shown in Figs. 4c$_1$, c$_2$, the concentrations of NO_2–N both increased in the DS during the operation of both systems due to the fact that the rejection of the FO membrane for nitrogen was not high. But NO_2–N concentration was low and inclined to be stable in the IERs-OMBR-MD system during the period time with the IERs addition, which may be because of the adsorption effect of 201×7 on NO_2^-. The relatively low concentrations of NO_2^- and high concentrations of NO_3^- both in the BR and DS implicated that the activity of nitrobacteria (NOB) may be not inhibited by high salinity.

Whatever, the combination of the activated sludge treatment with the dual high-retention membrane barriers (FO and MD) ensured the high removals of organic matters and nutrients by the OMBR-MD hybrid system.

3.3. Sludge characteristics

Fig. 5 shows the discernible differences in biomass characteristics during the IERs-OMBR-MD and OMBR-MD operating periods. Although no waste sludge was discharged during the operation periods, there was still a remarkable decrease in biomass concentration in both systems. This phenomenon may be due to that the increases in pH value inhibited the growth of microorganisms, and even caused some microorganisms death. In addition, an initial decrease but a subsequent increase occurred in SOUR. These experimental results are consistent with those of previous studies that salinity build-up inhibits microbial growth and activity by causing cell wall decomposition during OMBR operation [48,49]. Although the IERs-OMBR-MD hybrid system induced less significant salt accumulation in the BR than the OMBR-MD system (Fig. 2), MLSS and MLVSS in the IERs-OMBR-MD hybrid system were lower. The reason may be that the negatively charged sludge flocs were adsorbed and damaged by the cation exchange resins, and the complexed metal cations on the surface of bridged sludge particles were captured by some anions in the water phase, forming inorganic precipitation. However, a slight decrease in microbial activity did not affect the degradation of organic matters, and the adsorption and co-precipitation of resins also helped to enhance the contaminant removals. MLVSS/MLSS can reflect the concentration of inorganic

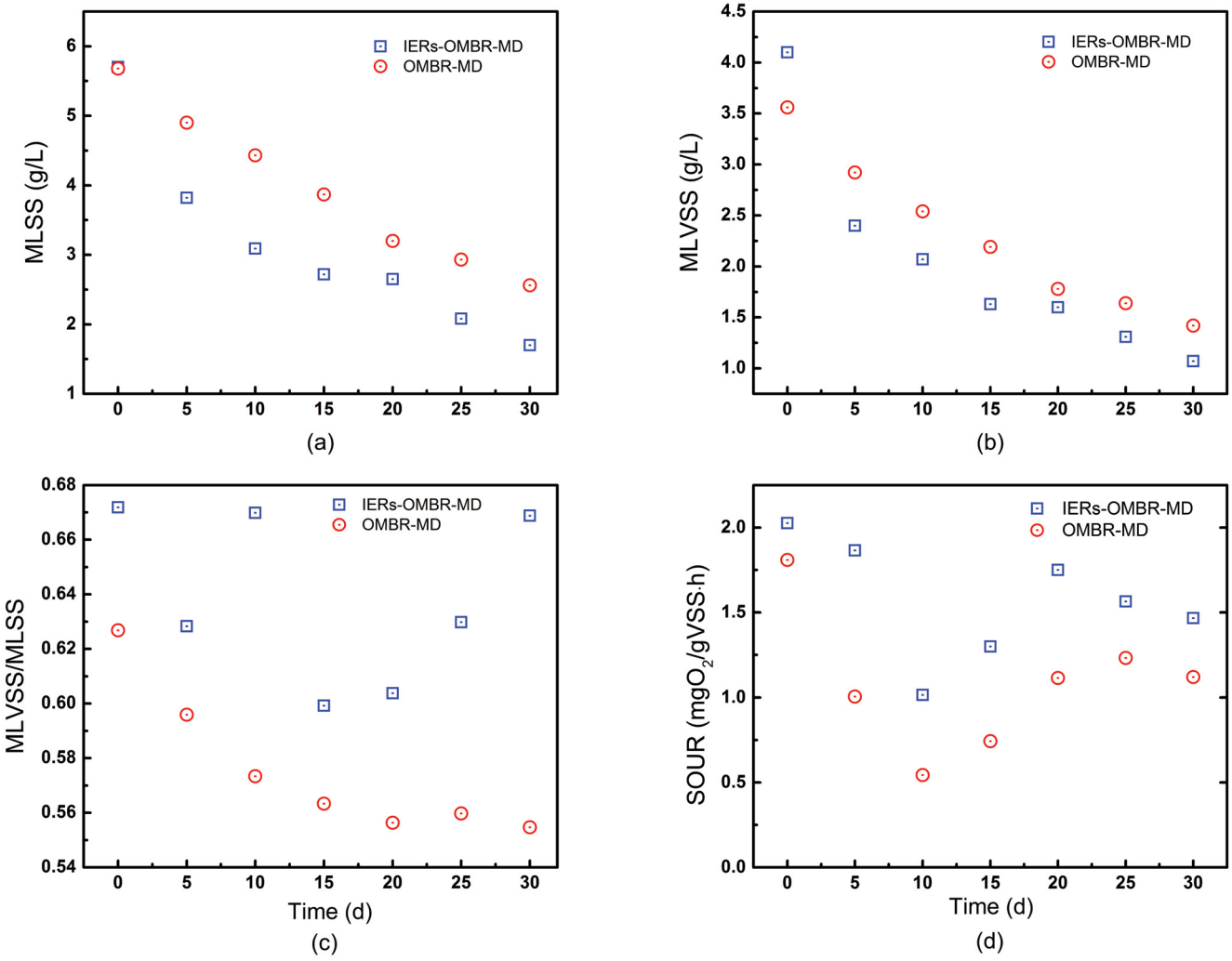

Fig. 5. Sludge characteristics in the IERs-OMBR-MD and OMBR-MD.

compounds in the mixed liquor. The lower MLVSS/MLSS value means that, the higher concentration of inorganic compounds accumulated and the more serious impact worked on biomass activity. The values of MLVSS/MLSS in the IERs-OMBR-MD system were higher than that in the OMBR-MD system, suggesting that the percentage of active biomass was higher in the IERs-OMBR-MD system.

From the variations of MLSS and MLVSS, the sludge concentrations of both OMBR-MD systems did not reach steady states after 30 d of operation, and long-term operation should be considered.

As shown in Fig. 6a–c, the variations of SMP, LB-EPS and TB-EPS in both systems were almost the same. At the beginning of the experiment, due to the high water flux and the reverse diffusion of draw solutes, the salinity in the BR increased, and the microorganisms released a large amount of SMP to protect themselves. Gradually, possibly because the microbes became acclimatized to the saline environment, they degraded most SMP and extracellular polymer substance (EPS). Zhang et al. found that SMP and EPS concentrations prone to be stable when the flux of OMBR tends to be steady, after continuous operation [50]. The microbial response to the saline environment resulted in more SMP and EPS released in the BR, which could aggravate the fouling of the FO membrane. We found that the SMP, LB-EPS and TB-EPS concentrations in the IERs-OMBR-MD hybrid system were almost lower than those in the traditional OMBR-MD system, probably because the IERs can adsorb proteins and polysaccharides in the BR (Fig. S3).

As shown in Fig. 6d, the zeta potentials of the mixed liquor in the IERs-OMBR-MD and OMBR-MD systems both declined. At the beginning of the experiment, the sludge zeta potentials of the IERs-OMBR-MD and OMBR-MD were –12.9 and –11.52 mV, respectively, and at the end of the experiment, the sludge zeta potentials were –29.43 and –22.5 mV, respectively, indicating that the negative charges of the sludge particles increased, which may cause the electrostatic repulsion between the flocs to increase, and the floc particles cannot destabilize and aggregate to form large sludge flocs. Otherwise, the surface of the FO membrane is also negatively charged, and there is also electrostatic repulsion between the sludge particles and the membrane surface. So, the increase of the negative charges

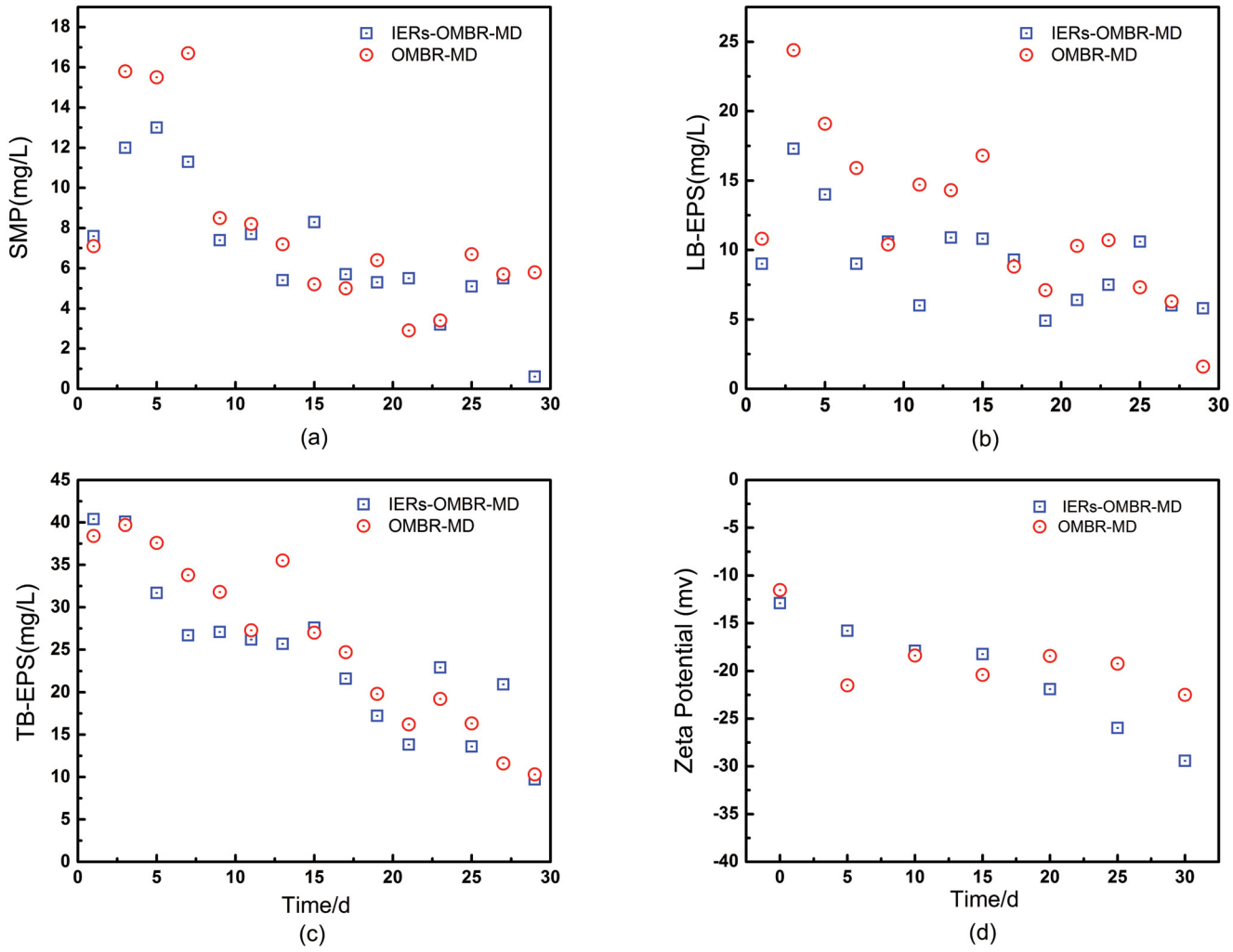

Fig. 6. SMP, LB-EPS, TB-EPS and zeta potential variations in the IERs-OMBR-MD and OMBR-MD.

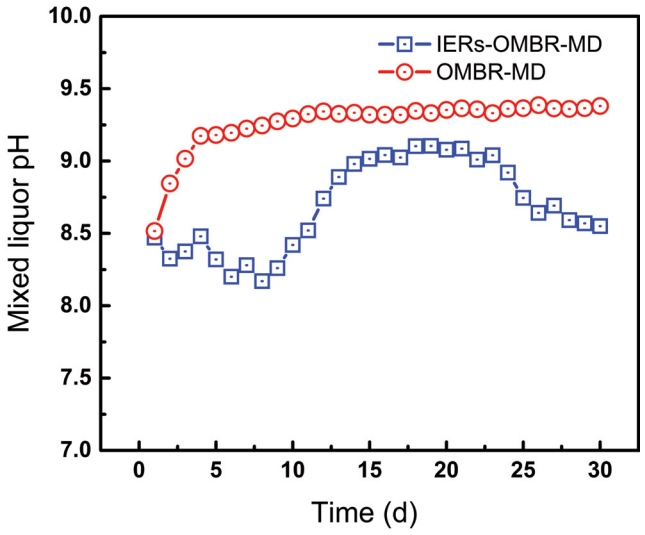

Fig. 7. Variations of mixed liquor pH values in the IERs-OMBR-MD and OMBR-MD.

may also reduce the tendency of sludge to be adsorbed on the FO membrane surface.

As shown in Fig. 7, the mixed liquor in both BRs was alkaline. Due to the consumption of alkalinity in biological nitrification, the alkalinity of the mixed liquor is favorable for nitrification. Therefore, NH_4^+–N had a high removal efficiency in the BR and NO_3^-–N accumulated significantly in the OMBR. The pH value of the mixed liquor increased from 8.5 to 9.3 during the first 10 d of the conventional OMBR-MD operation. This increase is due to the forward diffusion of protons from the BR into the DS, while sodium ions are transported in reverse to keep the BR electrically neutral [18]. The pH value of the mixed liquor tended to be stable as the water flux decreased (Fig. 2). In contrast, the pH value of the mixed liquor in the IERs-OMBR-MD system decreased from 8.47 to 8.26 during the first 10 d and from 9.0 to 8.5 during the final 10 d, respectively. The reason for this decrease was that when the ratio of anion and cation exchange resins was 3:1, the exchange capacity of the D001 resins was higher and more H^+ ions were generated. In the IERs-OMBR-MD system, the mixed

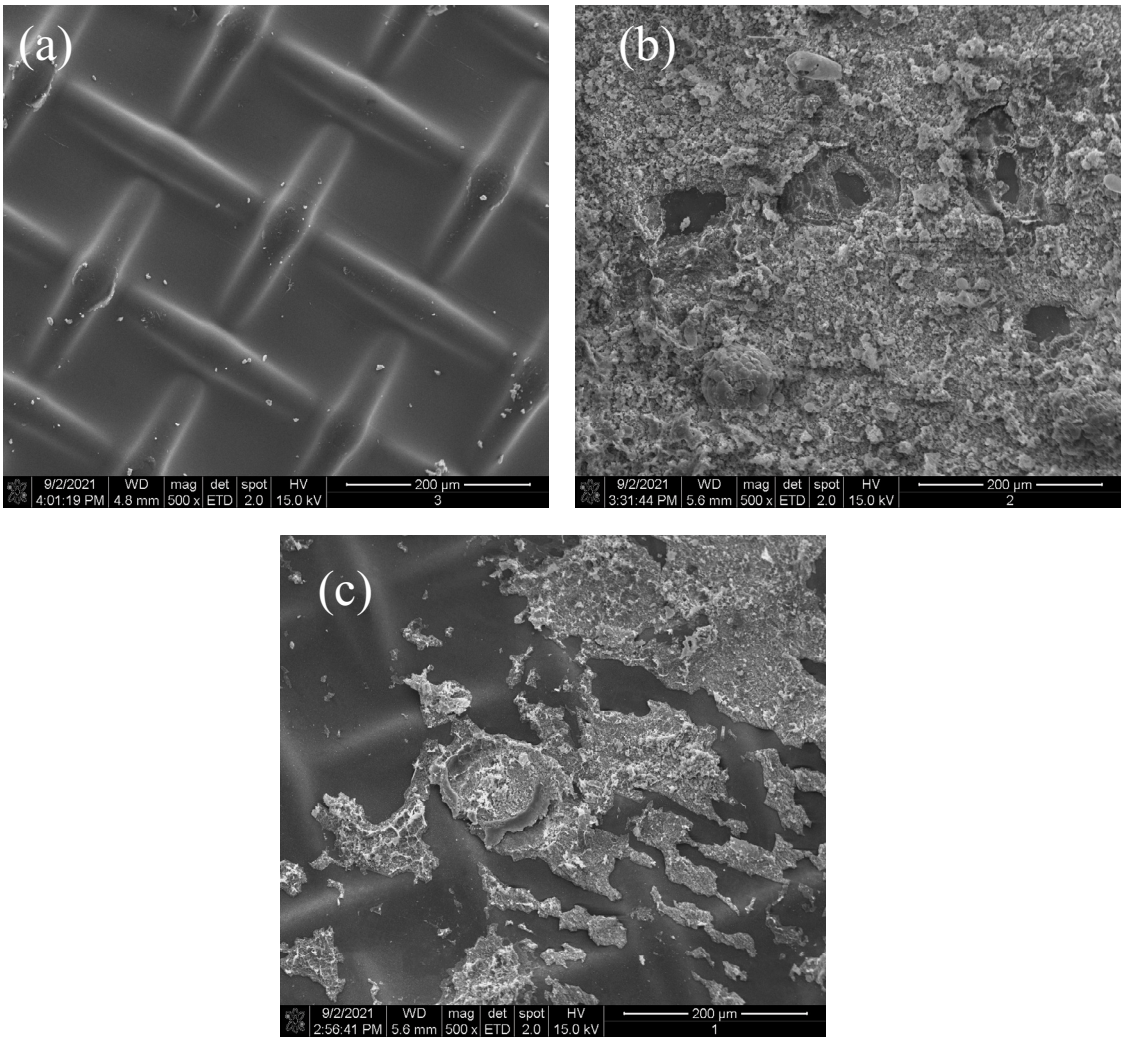

Fig. 8. SEM images of the FO membranes: (a) virgin membrane, (b) fouled membrane in the OMBR-MD and (c) fouled membrane in the IERs-OMBR-MD.

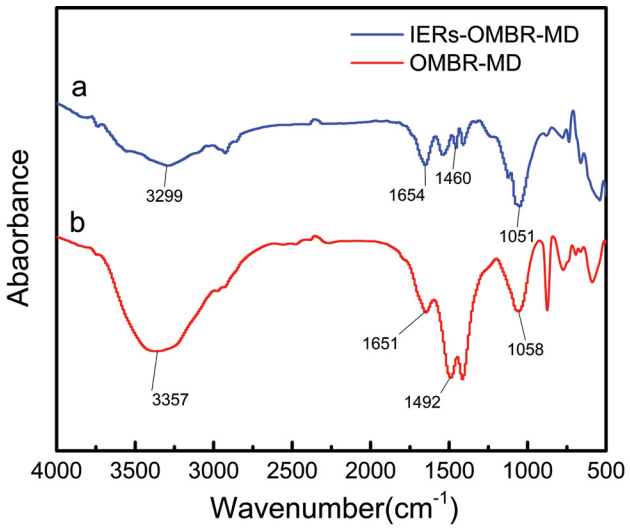

Fig. 9. FTIR absorption spectrums of the FO membrane surface contaminants in the IERs-OMBR-MD and OMBR-MD.

IERs can avoid the damage of high pH value to microbial activity and FO membrane performance.

3.4. Membrane fouling

The SEM images of virgin and fouled FO membranes in the IERs-OMBR-MD and OMBR-MD are shown in Fig. 8. The FO membrane surface of the OMBR-MD system was covered with a dense filter cake layer. However, the FO membrane surface of the IERs-OMBR-MD system was relatively smooth, and the membrane surface structure remained noticeable. Zhang et al stated that the contamination mainly happened on the FO membrane surface instead of in the internal pores [51]. The cake layer greatly enhances ECP, which increases the membrane fouling resistance and directly reduces the water permeability [52]. The IERs may adsorb proteins and carbohydrates in the BR and reduce the organic fouling on the membrane surface. In addition, only C and O present on the surface of the virgin FO membrane, while C, N, O, Na, Mg, Al, Si, P, Cl, K, Ca and other elements can be found on the surface of the fouled membrane (Fig. S4). The weight fraction distribution of all the elements on the fouled FO membrane is listed in Table S2. In the OMBR-MD system, the proportion of C is 30.33%, N 3.82%, O 44.64%, Na 3.08%, Mg 0.83%, Al 1.05%, Si 0.14%, P 6.2%, Cl 2.22%, K 0.01%, and Ca 7.00%. In the IERs-OMBR-MD system, the proportion of C was 23.76%, O 59.58%, Na 0.66%, Mg 0.99%, Al 0.18%, Si 0.28%, P 2.11%, Cl 0.47%, and Ca 11.9%. The lower percentages of C, N, P, Na, Cl in the IERs-OMBR-MD system may be attributed to the fact that the IERs adsorbed organic matters, nutrients and salts in the BR. The high rejection of FO membranes may be the cause of inorganic scale on the membrane surface.

As shown in Fig. 9, there were no significant differences in FTIR spectrums between the IERs-OMBR-MD and OMBR-MD. The wide peak at 3,299 cm^{-1} (3,357 cm^{-1}) may be the hydroxyl (–OH) bond stretching vibration. The designation of the 1,051 cm^{-1} (1,058 cm^{-1}) waveband associated with carbonyl (C=O) bonds indicates the possibility of polysaccharose. The peak at 1,492 cm^{-1} (1,460 cm^{-1}) proved the existence of amide II (C=N) bonds. The waveband at 1,654 cm^{-1} (1,651 cm^{-1}) was assigned to carbonyl and/or amide I (C=O) bonds and/or alkene (C=C) bonds which indicated the presence of the secondary proteins [53]. The results showed that the main components of the FO membrane surface foulants may be protein and polysaccharide, which are also the main components of EPS and SMP. The contents of polysaccharide, protein and TOC of the foulants from an area of 2 cm × 2 cm on the FO membrane were quantitatively analyzed. The contents of polysaccharide, protein and TOC in the IERs-OMBR-MD system were 32.5, 30.0 and 81.8 mg/L, and were 55.0, 37.5 and 111.3 mg/L in the OMBR-MD system. The FO membrane surface foulants of the IERs-OMBR-MD system were lower than those of the traditional OMBR-MD system, which was consistent with the results obtained from the SEM characterization.

3.5. Characterization of the recovered IERs

As shown in Fig. 10, the surfaces of 201×7 and D001 changed after adsorption in the IERs-OMBR-MD system. The surface of original 201×7 was quite smooth with a few hollow areas (a_1, a_2), but a large proportion of asperities on the 201×7 surface were observed after adsorption (b_1, b_2). According to the EDS diagram, in addition to C, O and N of original 201×7 composition, Cl and Ca were also found, because OH^- was replaced by Cl^- on the resins surface, and complexed Ca^{2+} was adsorbed on the resins surface (Fig. S5). The surface of original D001 has a large number of micro pores before adsorption, but the pores reduced after adsorption, and a large number of sediments covered the surface. In addition to C, O and S of original D001 composition, Na, Mg, K and Ca also appeared. H^+ of D001 was replaced by Na^+, Mg^{2+}, K^+ and Ca^{2+} (Fig. S5). This indicates that some inorganic and organic matters in the BR covered the IERs surface and reduced the FO membrane fouling.

As shown in Fig. 11, with the increase of initial salinity, the IERs desalting efficiency gradually decreased. When the concentration of TDS is between 100 and 400 mg/L, the desalting efficiency of the reclaimed IERs can still reach more than 99%. When the concentration of TDS is higher than 400 mg/L, the desalting efficiency decreased linearly. When the concentration of TDS is 1,000 mg/L, the desalting efficiency decreased to 30.09%. Compared with the data in Fig. S6, it can be found that the desalting efficiency of the reclaimed IERs significantly reduced, but still high at low salinities, indicating that the reclaimed resins can be used for the treatment of low salinity wastewater. IERs have strong recovery properties confirmed in previous studies [33,54].

4. Conclusion

This paper investigated the mitigation of salinity build-up in the bioreactor using IERs during the OMBR operation.

- Adding 8 g/L of the mixed IERs to the bioreactor can maintain a relatively low conductivity of 6.87 mS/cm, which was

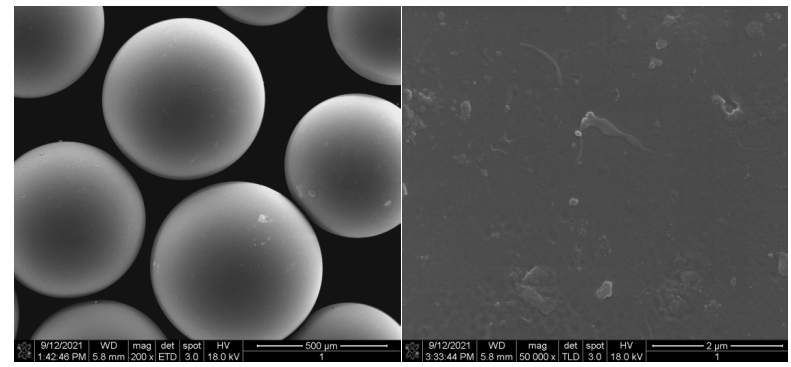

(a_1) (a_2)

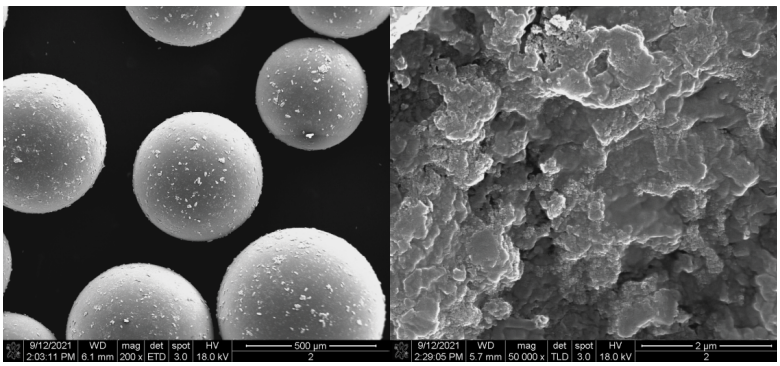

(b_1) (b_2)

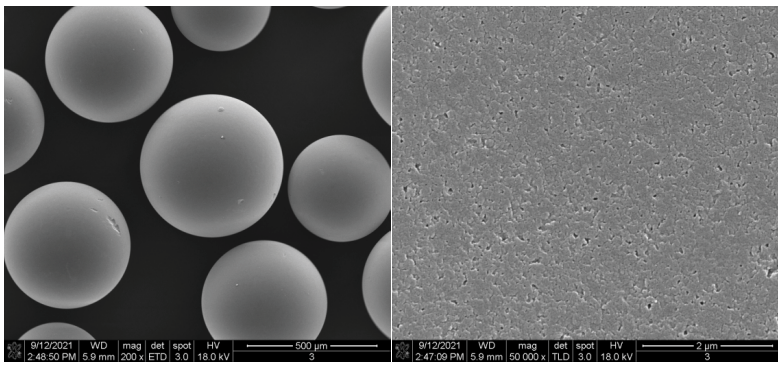

(c_1) (c_2)

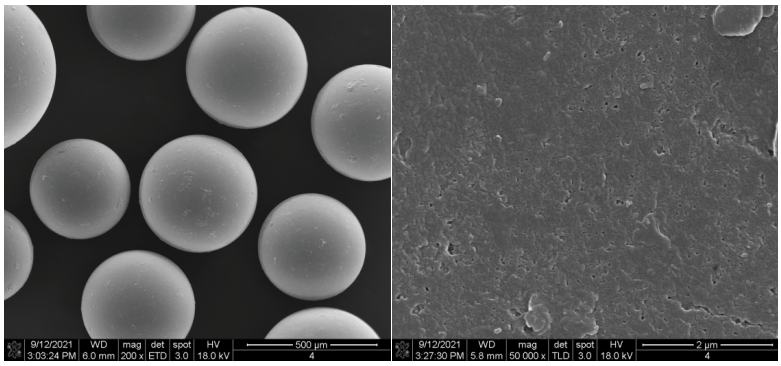

(d_1) (d_2)

Fig. 10. SEM images of the surfaces of 201×7 and D001 exchange resins. Before adsorption 201×7 resins; (a_1 and a_2, magnification 500 and 2 μm, respectively); Before adsorption D001 resins (c_1, c_2, magnification 500 and 2 μm, respectively); After adsorption 201×7 resins (b_1, b_2, magnification 500 and 2 μm, respectively); After adsorption D001 resins (d_1, d_2, magnification 500 and 2 μm, respectively).

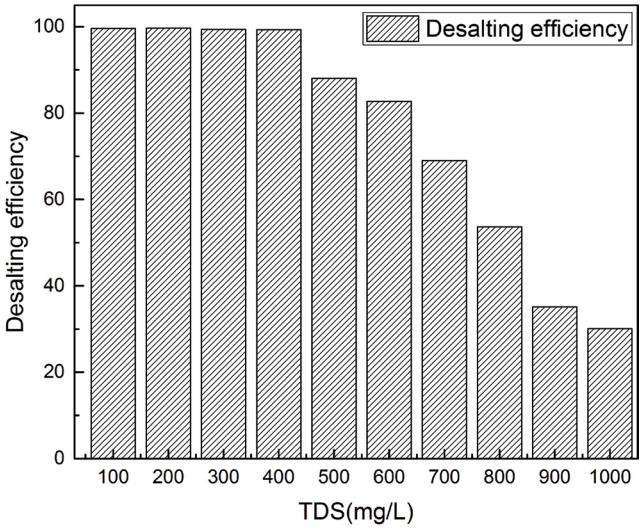

Fig. 11. Static adsorption data of the reclaimed resins at different initial salinities (taking the adsorption of sodium chloride solution as an example).

30% lower than that of the conventional OMBR-MD during 30 d of operation. It also increased the FO water flux.

- The IERs-OMBR-MD hybrid system ensures high removal efficiencies of organic matters and nutrients.
- The IERs-OMBR-MD hybrid system can avoid the damage of high pH value to microbial activity and membrane performance, and has significantly less fouling to the FO membrane.

These results suggest that ion-exchange resins have the potential to be applied to OMBR system. However, further studies to evaluate any adverse impact of IERs on sludge characteristics and FO membrane performance during long-term operation are recommended.

Acknowledgments

The research was supported by the Natural Science Foundation of Inner Mongolia (grant number 2021MS02020) and the Doctoral Foundation of Inner Mongolia University of Technology (grant number BS2020043).

References

[1] J.-Y. Lu, X.-M. Wang, H.-Q. Liu, H.-Q. Yu, W.-W. Li, Optimizing operation of municipal wastewater treatment plants in China: the remaining barriers and future implications, Environ. Int., 129 (2019) 273–278.
[2] Y.D. Xie, Q.H. Zhang, M. Dzakpasu, Y.C. Zheng, Y. Tian, P.K. Jin, S.J. Yang, X.C. Wang, Towards the formulation of rural sewage discharge standards in China, Sci. Total Environ., 759 (2021) 143533, doi: 10.1016/j.scitotenv.2020.143533.
[3] L. Chen, J. Chang, Y. Wang, A. Guo, Y. Liu, Q. Wang, Y. Zhu, Y. Zhang, Z. Xie, Disclosing the future food security risk of China based on crop production and water scarcity under diverse socioeconomic and climate scenarios, Sci. Total Environ., 790 (2021) 148110, doi: 10.1016/j.scitotenv.2021.148110.
[4] J. Zhang, K. Xiao, X. Huang, Full-scale MBR applications for leachate treatment in China: practical, technical, and economic features, J. Hazard. Mater., 389 (2020) 122138, doi: 10.1016/j.jhazmat.2020.122138.
[5] L. Goswami, R. Vinoth Kumar, S.N. Borah, N. Arul Manikandan, K. Pakshirajan, G. Pugazhenthi, Membrane bioreactor and integrated membrane bioreactor systems for micropollutant removal from wastewater: a review, J. Water Process Eng., 26 (2018) 314–328.
[6] M. Aslam, R. Ahmad, J. Kim, Recent developments in biofouling control in membrane bioreactors for domestic wastewater treatment, Sep. Purif. Technol., 206 (2108) 297–315.
[7] J. Ma, R. Dai, M. Chen, S.J. Khan, Z. Wang, Applications of membrane bioreactors for water reclamation: micropollutant removal, mechanisms and perspectives, Bioresour. Technol., 269 (2018) 532–543.
[8] B. Kim, G. Gwak, S. Hong, Review on methodology for determining forward osmosis (FO) membrane characteristics: water permeability (A), solute permeability (B), and structural parameter (S), Desalination, 422 (2017) 5–16.
[9] D.-J. Lee, M.-H. Hsieh, Forward osmosis membrane processes for wastewater bioremediation: research needs, Bioresour. Technol., 290 (2019) 121795, doi: 10.1016/j.biortech.2019.121795.
[10] Q. She, R. Wang, A.G. Fane, C.Y. Tang, Membrane fouling in osmotically driven membrane processes: a review, J. Membr. Sci., 499 (2016) 201–233.
[11] A. Tiraferri, N.Y. Yip, A.P. Straub, S. Romero-Vargas Castrillon, M. Elimelech, A method for the simultaneous determination of transport and structural parameters of forward osmosis membranes, J. Membr. Sci., 444 (2013) 523–538.
[12] X. Wang, V.W.C. Chang, C.Y. Tang, Osmotic membrane bioreactor (OMBR) technology for wastewater treatment and reclamation: advances, challenges, and prospects for the future, J. Membr. Sci., 504 (2016) 113–132.
[13] B. Yuan, X. Wang, C. Tang, X. Li, G. Yu, In situ observation of the growth of biofouling layer in osmotic membrane bioreactors by multiple fluorescence labeling and confocal laser scanning microscopy, Water Res., 75 (2015) 188–200.
[14] R.W. Holloway, A.S. Wait, A. Fernandes da Silva, J. Herron, M.D. Schutter, K. Lampi, T.Y. Cath, Long-term pilot scale investigation of novel hybrid ultrafiltration-osmotic membrane bioreactors, Desalination, 363 (2015) 64–74.
[15] X. Song, M. Xie, Y. Li, G. Li, W. Luo, Salinity build-up in osmotic membrane bioreactors: causes, impacts, and potential cures, Bioresour. Technol., 257 (2018) 301–310.
[16] G. Qiu, Y.-P. Ting, Osmotic membrane bioreactor for wastewater treatment and the effect of salt accumulation on system performance and microbial community dynamics, Bioresour, Technol., 150 (2013) 287–297.
[17] W.C. Lay, Y. Liu, A.G. Fane, Impacts of salinity on the performance of high retention membrane bioreactors for water reclamation: a review, Water Res., 44 (2010) 21–40.
[18] W. Luo, F.I. Hai, W.E. Price, M. Elimelech, L.D. Nghiem, Evaluating ionic organic draw solutes in osmotic membrane bioreactors for water reuse, J. Membr. Sci., 514 (2016) 636–645.
[19] K.S. Bowden, A. Achilli, A.E. Childress, Organic ionic salt draw solutions for osmotic membrane bioreactors, Bioresour. Technol., 122 (2012) 207–216.
[20] N.C. Nguyen, S.-S. Chen, H.T. Nguyen, S.S. Ray, H.H. Ngo, W. Guo, P.-H. Lin, Innovative sponge-based moving bed–osmotic membrane bioreactor hybrid system using a new class of draw solution for municipal wastewater treatment, Water Res., 91 (2016) 305–313.
[21] Y.-L. Yang, Z. He, Y. Wu, X.-L Yang, Y. Cai, H.-L. Song, Bioelectrochemically assisted osmotic membrane bioreactor with reusable polyelectrolyte draw solutes, Bioresour. Technol., 296 (2020) 122352, doi: 10.1016/j.biortech.2019.122352.
[22] J. Kim, J. Kim, J. Lim, S. Hong, Evaluation of ethanol as draw solute for forward osmosis (FO) process of highly saline (waste) water, Desalination, 456 (2019) 23–31.
[23] Z. Yang, X.-H. Ma, C.Y. Tang, Recent development of novel membranes for desalination, Desalination, 434 (2018) 37–59.
[24] W. Luo, M. Xie, X. Song, W. Guo, H.H. Ngo, J.L. Zhou, L.D. Nghiem, Biomimetic aquaporin membranes for osmotic membrane bioreactors: membrane performance and contaminant removal, Bioresour. Technol., 249 (2018) 62–68.

[25] D. Xiao, C.Y. Tang, J. Zhang, W.C.L. Lay, R. Wang, A.G. Fane, Modeling salt accumulation in osmotic membrane bioreactors: implications for FO membrane selection and system operation, J. Membr. Sci., 366 (2011) 314–324.
[26] X. Wang, Y. Chen, B. Yuan, X. Li, Y. Ren, Impacts of sludge retention time on sludge characteristics and membrane fouling in a submerged osmotic membrane bioreactor, Bioresour. Technol., 161 (2014) 340–347.
[27] W. Zhu, X. Wang, Q. She, X. Li, Y. Ren, Osmotic membrane bioreactors assisted with microfiltration membrane for salinity control (MF-OMBR) operating at high sludge concentrations: performance and implications, Chem. Eng. J., 337 (2018) 576–583.
[28] X. Wang, Y. Zhao, X. Li, Y. Ren, Performance evaluation of a microfiltration-osmotic membrane bioreactor (MF-OMBR) during removing silver nanoparticles from simulated wastewater, Chem. Eng. J., 313 (2017) 171–178.
[29] X. Wang, B. Yuan, Y. Chen, X. Li, Y. Ren, Integration of microfiltration into osmotic membrane bioreactors to prevent salinity build-up, Bioresour. Technol., 167 (2014) 116–123.
[30] G. Qiu, Y.M. Law, S Das, Y.P. Ting, Direct and complete phosphorus recovery from municipal wastewater using a hybrid microfiltration-forward osmosis membrane bioreactor process with seawater brine as draw solution, Environ. Sci. Technol., 49 (2015) 6156–6163.
[31] Y. Lu, Z. He, Mitigation of salinity buildup and recovery of wasted salts in a hybrid osmotic membrane bioreactor-electrodialysis system, Environ. Sci. Technol., 49 (2015) 10529–10535.
[32] N.D. Viet, S.-J. Im, C.-M. Kim, A. Jang, An osmotic membrane bioreactor–clarifier system with a deep learning model for simultaneous reduction of salt accumulation and membrane fouling, Chemosphere, 272 (2021) 129872, doi: 10.1016/j.chemosphere.2021.129872.
[33] H. Zhang, Y. Li, B. Cheng, C. Ding, Y. Zhang, Synthesis of a starch-based sulfonic ion exchange resin and adsorption of dyestuffs to the resin, Int. J. Biol. Macromol., 161 (2020) 561–572.
[34] E. Çermikli, F. Şen, E. Altıok, J. Wolska, P. Cyganowski, N. Kabay, M. Bryjak, M. Arda, M. Yüksel, Performances of novel chelating ion exchange resins for boron and arsenic removal from saline geothermal water using adsorption-membrane filtration hybrid process, Desalination, 491 (2020) 114504, doi: 10.1016/j.desal.2020.114504.
[35] X. Yang, K. Wang, H. Wang, J. Zhang, Z. Mao, Novel process combining anaerobic-aerobic digestion and ion exchange resin for full recycling of cassava stillage in ethanol fermentation, Waste Manage., 62 (2017) 241–246.
[36] Y. Jia, L. Ding, P. Ren, M. Zhong, J. Ma, X. Fan, Performances and mechanism of Methyl orange and Congo red adsorbed on the magnetic ion-exchange resin, J. Chem. Eng. Data, 65 (2020) 725–736.
[37] K. Chen, X. Wang, X. Li, J. Qian, X. Xiao, Impacts of sludge retention time on the performance of submerged membrane bioreactor with the addition of calcium ion, Sep. Purif. Technol., 82 (2011) 148–155.
[38] Q. Wang, Z. Wang, Z. Wu, X. Han, Sludge reduction and process performance in a submerged membrane bioreactor with aquatic worms, Chem. Eng. J., 172 (2011) 929–935.
[39] J. Lee, W.-Y. Ahn, C.-H. Lee, Comparison of the filtration characteristics between attached and suspended growth microorganisms in submerged membrane bioreactor, Water Res., 35 (2001) 2435–2445.
[40] M. DuBois, K.A. Gilles, J.K. Hamilton, P.A. Rebers, F. Smith, Colorimetric method for determination of sugars and related substances, Anal. Chem., 28 (1956) 350–356.
[41] L. Yang, J. Xu, Y. Huang, L. Li, P. Zhao, L. Lu, X. Cheng, D. Zhang, Y. He, Using layered double hydroxides and anion exchange resin to improve the mechanical properties and chloride binding capacity of cement mortars, Constr. Build. Mater., 272 (2021) 122002, doi: 10.1016/j.conbuildmat.2020.122002.
[42] Y. Zhang, B. Pan, C. Shan, X. Gao, Enhanced phosphate removal by nanosized hydrated La(III) oxide confined in cross-linked polystyrene networks, Environ. Sci. Technol., 50 (2016) 1447–1454.
[43] J. Zhang, C. Zhu, F. Zhou, L. Ma, Adsorption behavior and kinetics for L-valine separation from aqueous solution using ion exchange resin, React. Funct. Polym., 130 (2018) 51–60.
[44] G.J. Millar, S.J. Couperthwaite, S. Papworth, Ion exchange of sodium chloride and sodium bicarbonate solutions using strong acid cation resins in relation to coal seam water treatment, J. Water Process Eng., 11 (2016) 60–67.
[45] Y. Lin, Q. Chen, Y. Wang, K. Sua, T. Hao, Enhancing the water flux and biological treatment in bilateral influent submerged FOMBR via applying the strategy of intermittent discharging salt, Environ. Technol., 42 (2020) 3379–3389.
[46] W.C.L. Lay, Y. Liu, A.G. Fane, Impacts of salinity on the performance of high retention membrane bioreactors for water reclamation: a review, Water Res., 44 (2010) 21–40.
[47] R.W. Holloway, A.E. Childress, K.E. Dennett, T.Y. Cath, Forward osmosis for concentration of anaerobic digester centrate, Water Res., 41 (2007) 4005–4014.
[48] W. Luo, F.I. Hai, J. Kang, W.E. Price, W. Guo, H.H. Ngo, K. Yamamoto, L.D. Nghiem, Effects of salinity build-up on biomass characteristics and trace organic chemical removal: implications on the development of high retention membrane bioreactors, Bioresour. Technol., 177 (2015) 274–281.
[49] E. Reid, X. Liu, S.J. Judd, Effect of high salinity on activated sludge characteristics and membrane permeability in an immersed membrane bioreactor, J. Membr. Sci., 283 (2006) 164–171.
[50] B. Zhang, X. Song, L.D. Nghiem, G. Li, W. Luo, Osmotic membrane bioreactors for wastewater reuse: Performance comparison between cellulose triacetate and polyamide thin film composite membranes, J. Membr. Sci., 539 (2017) 383–391.
[51] J. Zhang, W.L.C. Loong, S. Chou, C. Tang, R. Wang, A.G. Fane, Membrane biofouling and scaling in forward osmosis membrane bioreactor, J. Membr. Sci., 403–404 (2012) 8–14.
[52] Q. She, X. Jin, Q. Li, C.Y. Tang, Relating reverse and forward solute diffusion to membrane fouling in osmotically driven membrane processes, Water Res., 46 (2012) 2478–2486.
[53] W. Luo, H.V. Phan, M. Xie, F.I. Hai, W.E. Price, M. Elimelech, L.D. Nghiem, Osmotic versus conventional membrane bioreactors integrated with reverse osmosis for water reuse: biological stability, membrane fouling, and contaminant removal, Water Res., 109 (2017) 122–134.
[54] W.-L. Wu, Z.-Q. Tan, G.-J. Wu, L. Yuan, W.-L. Zhu, Y.-L. Bao, L.-Y. Pan, Y.-J. Yang, J.-X. Zheng, Deacidification of crude low-calorie cocoa butter with liquid–liquid extraction and strong-base anion exchange resin, Sep. Purif. Technol., 102 (2013) 163–172.

Supplementary information

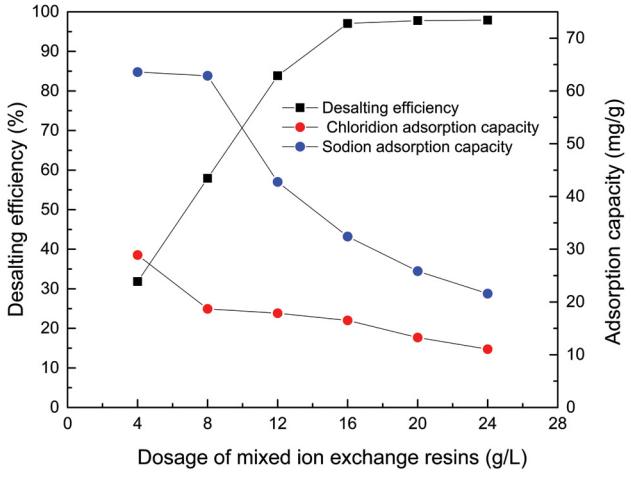

Fig. S1. Desalting efficiency of mixed ion-exchange resins with different dosage.

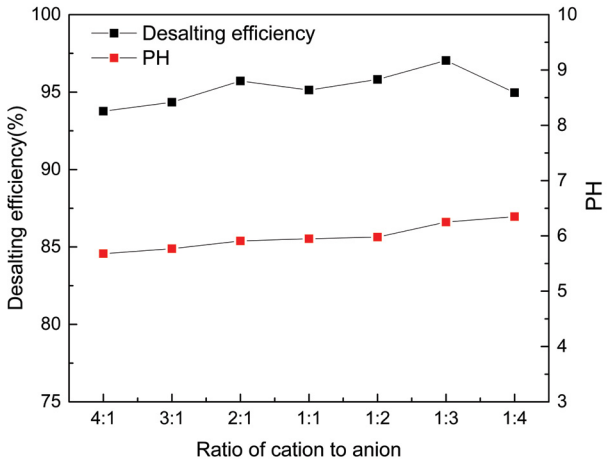

Fig. S2. Desalting efficiency of different cationic and anionic resin ratios.

Table S1
Compositions and concentration of synthetic domestic wastewater

Composition	Concentration (mg/L)
Glucose	267
Soluble starch	267
$NaHCO_3$	233
NH_4Cl	83
Peptone	17
KH_2PO_4	27
$MgCl_2$	3
$CaCl_2$	3
$FeCl_3$	3

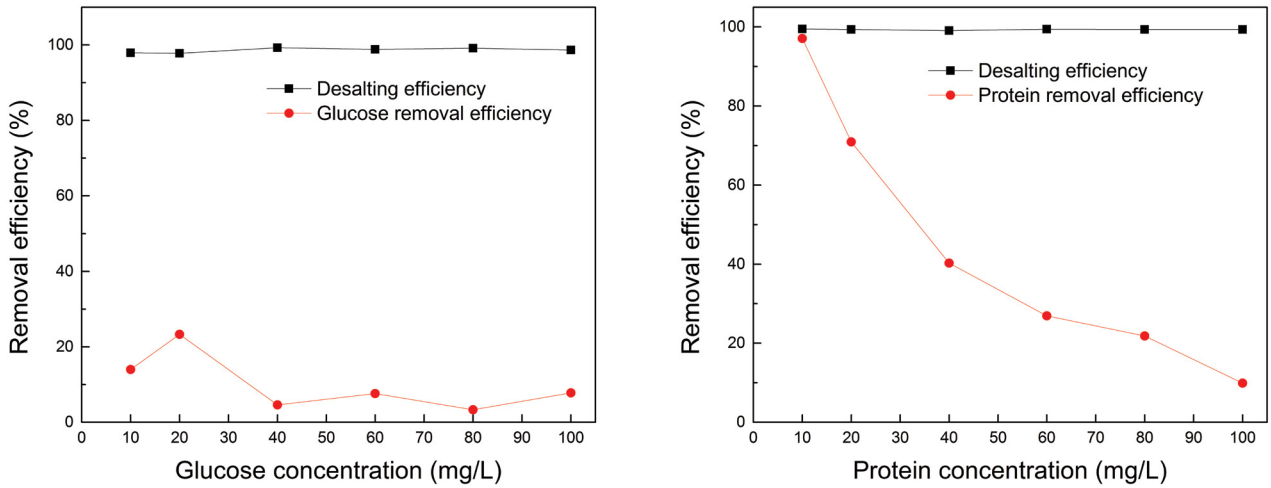

Fig. S3. Desalting efficiency of ion-exchange resin with different coexisting organics.

Table S2
Element weight distribution of foulants on fresh and fouled membrane surfaces in the OMBR by EDS analysis

Element wt.%	Virgin membrane	Fouled membrane in OMBR-MD	Fouled membrane in IERs-OMBR-MD
C	74.31	30.33	23.76
N	–	3.82	–
O	25.69	44.64	59.58
Na	–	3.08	0.66
Mg	–	0.83	0.99
Al	–	1.05	0.18
Si	–	0.82	0.28
P	–	6.20	2.11
Cl	–	2.22	0.47
K	–	0.01	–
Ca	–	7.00	11.9

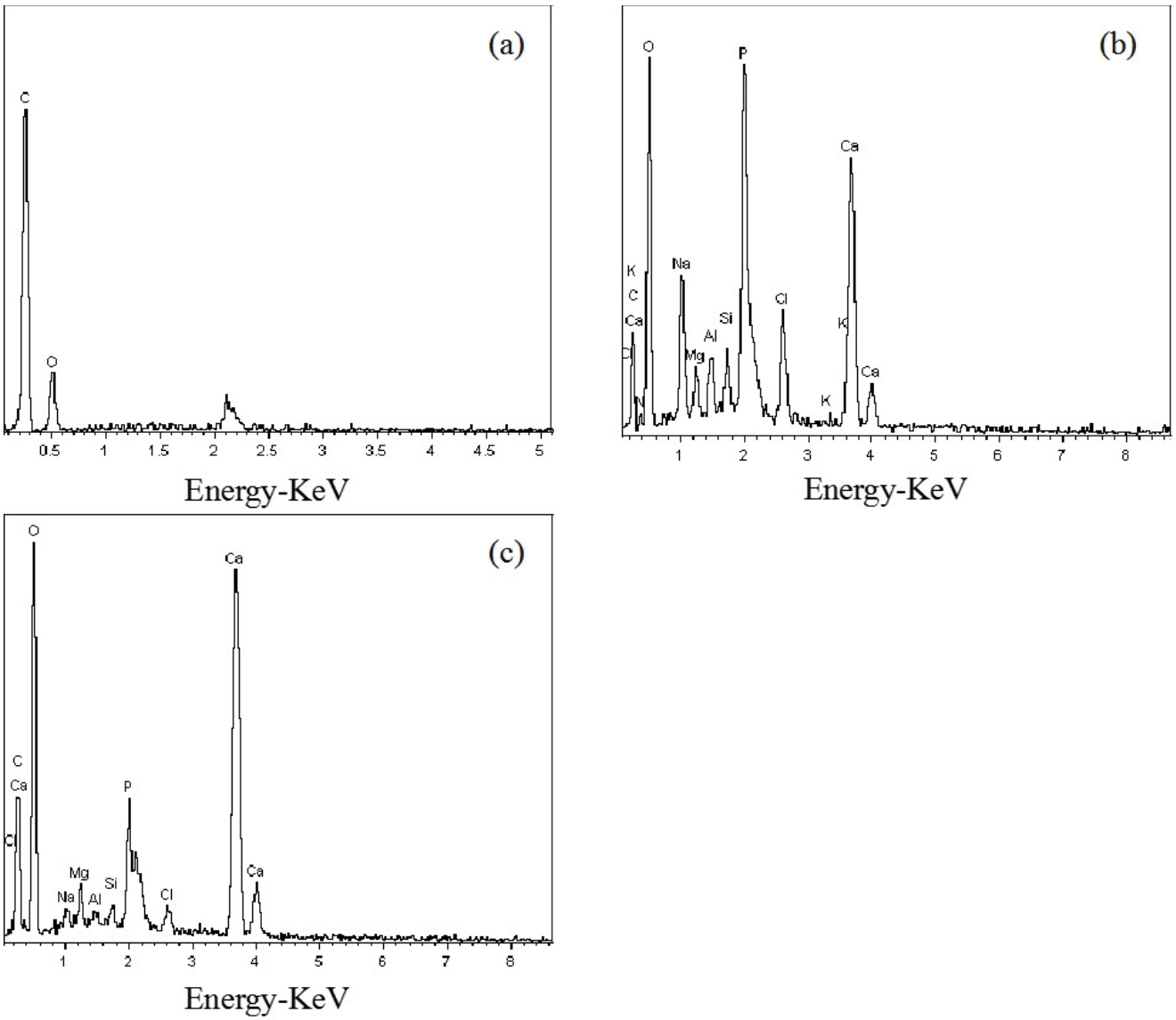

Fig. S4. EDS of the FO membrane: (a) virgin membrane, (b) fouled membrane in the OMBR-MD and (c) fouled membrane in the IERs-OMBR-MD.

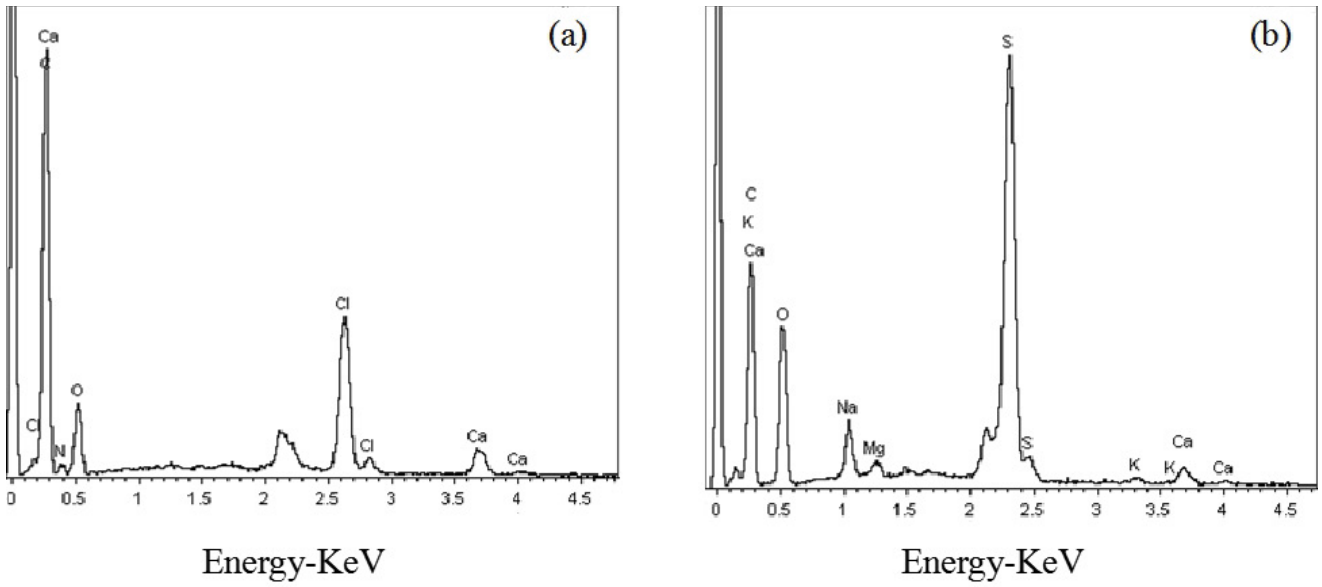

Fig. S5. EDS of the 201×7 and D001 anion exchange resins: (a) after adsorption 201×7 resin and (b) after adsorption D001 resin.

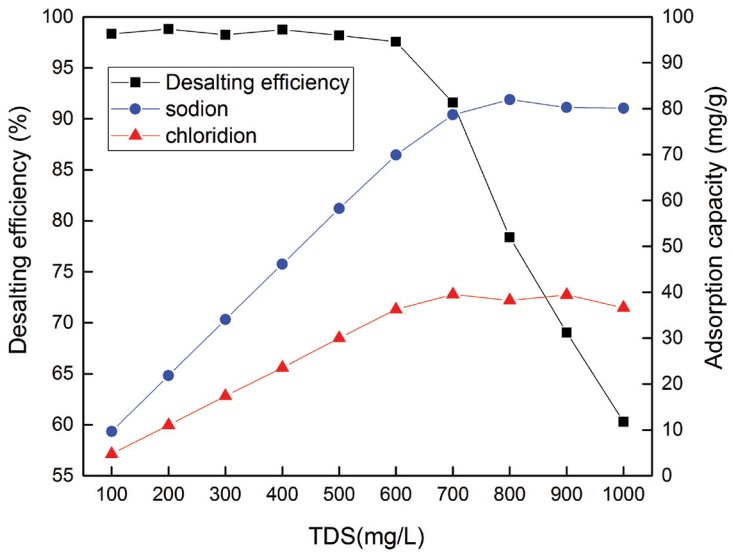

Fig. S6. Static adsorption of IERs at different salinities (taking adsorption of sodium chloride solution as an example). Experimental conditions: the dosage of mixed resin was 16 g/L, the ratio of positive anion was 1:3, the shock temperature of water bath was 25°C, the shock time was 2 h, and the speed was 150 r/min.